JARQ 60 (3), 231-239 (2026) https://www.jircas.go.jp

Evaluation of Unmanned Aerial Vehicle-Based Structure-from-Motion (UAV-SfM)-Derived Plant Height for Yield Estimation and Individual Selection in Cool-Season Grass Breeding

Miyu MAKISHIMA[1], Motohiro YOSHIMURA[2], Ryo FUJIWARA[2,3], Yasuharu SANADA[2], Yoshinori TAKAHARA[1] and Yukio AKIYAMA[2]*

[1] Materials Science and Bioengineering, Nagaoka University of Technology, Niigata, Japan
[2] Division of Dairy Production Research, Hokkaido Agricultural Research Center, National Agriculture and Food Research Organization, Sapporo, Japan
[3] BrainPad Inc., Tokyo, Japan

Abstract

Unmanned Aerial Vehicle-Structure from Motion (UAV-SfM) is a labor-saving method for measuring plant height and volume. Recent studies have explored yield estimation in various crops using plant height derived from UAV-SfM. This study examined the application of UAV-SfM in grass breeding, focusing on yield estimation for productivity testing trials and evaluating its potential for individual plant selection. Yield estimation in *Lolium perenne* was analyzed using Random Forest (RF) regression with UAV-SfM-estimated grass height, temperature, precipitation, and vegetation indices as predictor variables. The results indicated that, even under optimal conditions, the achieved accuracy was insufficient for direct application in breeding and productivity testing trials, highlighting the limitations of UAV-SfM for yield estimation at present. For individual selection, *Dactylis glomerata* was assessed by comparing individual plant heights derived from UAV-SfM to rG, an established index known to correlate with breeder scores. A strong positive correlation (r > 0.8) was observed between rG and UAV-SfM-estimated individual plant heights, suggesting that UAV-SfM-derived height is potentially useful for individual plant selection. Our findings suggest that while UAV-SfM shows potential for individual plant selection in grass breeding, further methodological refinement is required before it can be reliably employed for yield estimation.

Discipline: Agricultural Engineering
Additional key words: crop height model, random forest

Introduction

Livestock farming is a vitally important industry, with feed playing an indispensable role. In Japan, forage grasses contribute significantly to domestic feed production. However, the effects of abnormal weather and a declining agricultural workforce underscore the need for improved forage grass breeding and more efficient grassland management. The continuous development of new varieties is essential to meet changing demand. Currently, forage grass breeding evaluations rely heavily on manual assessments. However, the decreasing number of breeders and the time-consuming nature of fieldwork emphasize the need for labor-saving methods. Such methods would allow for the evaluation of more individuals, improving breeding efficiency. Additionally, the subjective nature of traditional assessments highlights the need for objective indicators. To address these challenges and achieve both efficiency and labor-saving in breeding, remote sensing technology is increasingly being explored.

Structure from Motion (SfM) is a remote sensing technique that creates three-dimensional (3D) point clouds by identifying common features in images from different viewpoints. This method can be used to derive a Crop Height Model (CHM), which represents plant height, by subtracting a Digital Terrain Model (DTM) from a Digital Surface Model (DSM). Using the CHM,

*Corresponding author: akiyama.yukio669@naro.go.jp
Received 13 May 2025; accepted 22 September 2025; J-STAGE Advanced Epub 30 April 2026.
https://doi.org/10.6090/jarq.24S07

plant height and volume can be estimated. Unmanned Aerial Vehicles (UAVs) are widely used for remote sensing data collection due to their low cost and ease of deployment. UAV-SfM has been used to estimate plant height and crop yields in a variety of agricultural contexts. For example, the prediction of yield based on UAV-SfM-estimated plant height has been investigated in several crops, including grass (Grüner et al. 2019), corn (Li et al. 2016), and barley (Bendig et al. 2015). Productivity testing trials, which involve yield studies, are a key step in grass breeding programs aimed at developing high-yielding varieties. Accurate yield prediction from UAV-SfM-derived grass height could significantly reduce labor requirements.

Individual selection is a critical step in grass breeding. Breeders visually assess individual plant growth to identify superior lines, but these evaluations are subjective and can vary among evaluators. In addition, since the labor and time required to perform these tasks increase significantly with larger populations, there is a need to develop objective, labor-saving methods. One such method is the use of vegetation indices calculated from image data, such as RGB values and near-infrared wavelengths. These indices provide an objective means of assessing plant growth status and are well-suited for labor-saving monitoring, as they can be derived from images without direct measurement. Although a correlation has been demonstrated between normalized difference vegetation index (NDVI) values, visual evaluations, and biomass in perennial ryegrass (Wang et al. 2019), applying NDVI requires expensive near-infrared cameras. Our research group proposed using the vegetation index rG, calculated from RGB aerial images (Akiyama et al. 2019). The rG index, which stands for the relative Green-Red Vegetation Index, represents the relative value of the Green-Red Vegetation Index (GRVI; Equation 1) and ranges from 0 to 100 (Equation 2). Strong correlations have been observed between breeders' evaluations and rG values. Moreover, progeny selected based on rG showed performance similar to or slightly better than that of progeny selected through visual evaluation (Kikawada et al. 2024).

$$\mathrm{GRVI} = (\mathrm{Green} - \mathrm{Red})/(\mathrm{Green} + \mathrm{Red}) \quad \ldots \text{(Equation 1)}$$

Green: Intensity of green light, Red: Intensity of red light

$$\mathrm{rG} = (\mathrm{GRVI} - \mathrm{GRVI_{min}})/(\mathrm{GRVI_{max}} - \mathrm{GRVI_{min}}) \times 100 \quad \ldots \text{(Equation 2)}$$

$\mathrm{GRVI_{max}}$: Maximum GRVI value within the analysis area of the same image

$\mathrm{GRVI_{min}}$: Minimum GRVI value within the analysis area of the same image

In individual selection evaluations, height and volume are key factors in addition to color information. Since larger plant size generally indicates better growth, it is hypothesized that individual growth conditions could be evaluated using UAV-SfM-estimated grass height derived from the CHM. This implies that a UAV-SfM-estimated grass height, such as rG, could be used as a labor-saving, objective evaluation method.

We attempted to apply UAV-SfM to evaluate grass breeding methods. First, we applied UAV-SfM to productivity testing trials to evaluate grass strains. Second, we compared UAV-SfM with the rG method for selecting valuable individuals. This paper focuses on the application of UAV-SfM to grass breeding. Specifically, it aims to evaluate the feasibility of UAV-SfM for estimating yield in productivity testing trials and for estimating individual plant height in individual selection, thereby assessing its potential for practical implementation in actual breeding programs. This was an experimental study to test the feasibility of existing breeding technology for field use, especially in Japan's cold regions, rather than methodical innovation.

Materials and methods

1. Yield estimation of *Lolium perenne*

(1) Target fields and drone data collection

Data were collected from *Lolium perenne* productivity testing fields for grazing use at the Hokkaido Agricultural Research Center (Hokkaido, Japan) from 2022 to 2023. An overview of the plots is shown in Figure 1. The field consisted of 20 plots, each with four rows of a single variety. Five varieties were randomly planted with four replicates. Each row was 4 m long, with a spacing of 30 cm. The field was sown in 2021, with the plants overwintering once by 2022 and twice by 2023. Ground control points (GCPs) for SfM processing were placed at the four corners of the field, and their coordinates were obtained using a high-precision global navigation satellite system (GNSS) mobile station (D-RTK2; SZ DJI Technology Co. Ltd., Shenzhen, China). Harvesting was conducted when the reference variety reached a height of 30 cm (measured by hand-stretching). Two harvests were conducted each year, referred to as the first and second harvests. In 2022, harvesting was performed eight times, and in 2023, six times. Wet and dry yields (wet yield: the weight measured immediately after harvest; dry yield: the weight after drying at 70°C for more than 2 days) were recorded for each plot (n = 20).

Aerial photography was conducted using a commercial UAV (Phantom 4 RTK, SZ DJI Technology Co. Ltd.) with an RGB camera (lens: 8.8 mm, sensor: 25.4 mm CMOS 20 megapixels). The UAV followed a grid flight path (80% forward overlap, 60% side overlap, 25 m altitude), and the camera angle was set to –60° (0° =

horizontal, –90° = nadir). Aerial photography was conducted on the day of harvesting or the preceding day.

(2) SfM and plant height estimation

SfM was performed using Agisoft Metashape Professional 2.1.2 (Agisoft LLC, St. Petersburg, Russia). A 3D point cloud, DEM, and orthomosaic image were generated from the image set captured on each shooting date. SfM settings are shown in Table 1. Height corrections were performed after image loading and alignment, using the positional information from field GCPs. Four GCPs placed around the field were primarily used, but when GCPs were obscured by weeds, three GCPs or those from neighboring fields were used. The DEM of the field after snowmelt (12 April 2022) was used as the DTM. The CHM was calculated in QGIS 3.34.8 (QGIS Association, Grüt, Switzerland) by subtracting the DTM from the DEM of each shooting date. The average plant height within analysis plots (0.6 × 3.2 m) was calculated from the CHM and used as the estimated plant height. Analysis plots were defined as the inner two rows of the total four rows for each variety, with a 10% margin on each side. Some studies suggested the 90th percentile of DEM in the analysis plot would be estimated plant height (Malambo et al. 2018, Galli et al. 2021). However, to examine the connection between plant height and yield over time, it is anticipated that using the mean estimated plant height would have minimal impact on the conclusion. Therefore, this study used the average DEM value at the analysis plot as the estimated plant height.

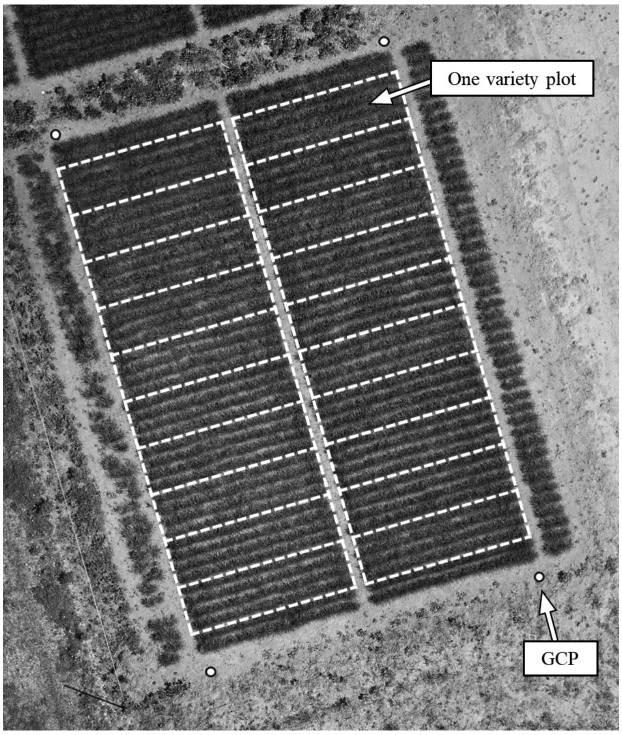

Fig. 1. Overview of the perennial ryegrass plots
Dashed lines indicate plots of each variety. Outside the dashed line are border areas, which are not included in the data analysis (non-assessed areas). Dots indicate GCPs located at the four corners.

(3) Yield estimation

Initial yield estimation was conducted using SfM-estimated plant height, precipitation, and temperature as explanatory variables. Weather data were sourced from the Web Meteorological Observatory System (https://meteo.db.naro.go.jp/), utilizing accumulated precipitation and average temperature between harvesting dates. For first cuttings, provisional weather data were calculated retroactively using average inter-harvest intervals. Subsequently, yield estimation was expanded to include a vegetation index as a fourth variable. The predictive performance of this four-variable model was compared with a three-variable model (plant height, temperature, precipitation) to assess the impact of the vegetation index. Nineteen vegetation indices,

Table 1. SfM parameter setting

Process	Parameter	Setting
Alignment	Accuracy	High
	Generic preselection	Yes
	Key point limit	40,000
	Tie point limit	4,000
Depth maps generation	Quality	High
	Filtering mode	Mild
DEM	Source data	Point cloud
	Interpolation	Enabled
Orthomosaic	Blending mode	Mosaic
	Surface	DEM
	Enable hole filing	Yes

reported to be correlated with breeder scores for disease severity and wintering ability ($r^2 \geq 0.5$) (Kikawada et al. 2022), were selected and calculated using RGB values extracted from orthomosaic images (Table 2).

In cases with many features or significant noise, Random Forest (RF) analysis may be more advantageous than algorithms such as Support Vector Machines (SVM) or Artificial Neural Networks (ANN). In fact, there were cases where RF achieved higher accuracy than SVM or ANN in biomass estimation and tree height estimation (Wang et al. 2016, da Silva et al. 2021). Therefore, RF analysis was performed to estimate yield using five distinct data partitioning methods in this study. The model was constructed with 100 decision trees, with no limit on tree depth and all available features considered at each split. A fixed random seed (random_state = 0) was applied to ensure reproducibility, and bootstrap sampling was used for tree construction. In single-year analyses (2022, 2023), data were randomly partitioned into five groups of four plots each. Four groups (16 plots) served as training data, and the remaining group (4 plots) served as test data. This procedure generated an RF model used to compute the coefficient of determination (R^2) and the mean absolute percentage error (MAPE) for the estimated yield. This process was repeated until all groups served once as test data. This resulted in five yield estimation models per partitioning method, with accuracy evaluated based on the average R^2 and MAPE. Two-year analyses (2022 and 2023) followed a similar approach, with plots designated as training data (16 plots/year) or test data (4 plots/year). The models were trained using the combined 32-plot training dataset and tested against an 8-plot test set. Five models were generated and evaluated based on the average R^2 and MAPE. Furthermore, a single-year training and testing approach was applied, in which the model was trained using data from one year (20 plots) and data from the other year (20 plots), with both combinations evaluated (2022→2023, 2023→2022).

Table 2. Vegetation index

Vegetation index	Definition
g	G / (R + G + B)
GmR	G – R
GmR_2	g – r
GRVI	(G – R) / (G + R)
MGVRI	$(G^2 – R^2) / (G^2 + R^2)$
VARI	(G – R) / (G + R – B)
GI	G / R
RGRI	R / G
ExG	2G – R – B
ExGR	(2G – R – B) - (1.4R– G)
ExR_2	1.4r – g
ExG_2	2g – r – b
GLI	(2G – R – B) / (2G + R + B)
CIVE	0.441R – 0.811G + 0.385B +18.78745
CIVE_2	0.441r – 0.811g + 0.385b +18.78745
SAVI	(1.5(G – R)) / (G + R + 0.5)
SAVI_2	(1.5(g – r)) / (g + r + 0.5)
RGVBI	$(G – (B * R)) / (G^2 + (B * R))$
RGBVI	$(G^2 – (R * B)) / (G^2 + (R * B))$

R, G, and B represent the RGB values of the image. r = R / (R + G + B), b = B / (R + G + B).
Vegetation index names and formulas partially derived from Kikawada et al. (2022).

2. UAV-SfM-estimated plant height for individual selection evaluation in *Dactylis glomerata*

Data collection was conducted in the *Dactylis glomerata* selection field at the Hokkaido Agricultural Research Center (Hokkaido, Japan) in 2023. The field contained 2,886 individuals. Aerial imaging was performed using a Phantom 4 RTK UAV on 1 May 2023 (DSM acquisition) and on 22 June 2023 (DTM acquisition, after harvest). The UAV followed a grid flight path (80% forward overlap, 60% side overlap, 25 m altitude, –60° camera angle), and aerial imaging for rG estimation was performed at an altitude of 40 m to capture the entire field in a single image. SfM was conducted for each set of aerial images using the same settings as in section 1-(2). It has been reported that combining aerial image sets for DTM and DSM during photo alignment, followed by separate SfM processing (co-alignment workflow), can correct baseline shifts (Cook & Dietze 2019). Since no GCPs were installed, GCP-based corrections were not done; instead, a co-alignment workflow was applied. In SfM processing using Agisoft Metashape Professional 2.1.2, the DSM and DTM image datasets were initially combined for photo alignment and camera optimization. The tie points generated from the combined DSM-DTM image dataset were then duplicated and used for subsequent SfM processing: one set was combined with the DSM image dataset to generate a DEM (treated as the DSM), and the other set was combined with the DTM image dataset to generate a DEM (treated as the DTM). The resulting DSM and DTM were imported into QGIS 3.34.8, and their difference was calculated to derive the CHM. Based on the CHM, the SfM-estimated average plant height for each *D. glomerata* individual was determined. Additionally, using an image of the field captured at an altitude of 40 m, the rG value for each individual was calculated using image analysis software

(Hojolook 1.0.2; National Agriculture and Food Research Organization (NARO), Japan). The SfM-estimated average plant height and rG values for each individual were then compared.

Results and discussion

1. Plant height estimation of *Lolium perenne*

Figure 2 shows the trend in average plant height (calculated from the CHM) alongside plots of SfM-estimated plant height, wet yield, and dry yield. The average SfM-estimated plant height ranged from approximately 9 to 18 cm, lower than the manually measured 30 cm at harvest. This discrepancy was likely attributable to factors such as lodging, the averaging effect of row and inter-row spaces, leaf movement during UAV imaging, and potential real-time kinematic-GNSS positioning errors.

Yield correlated positively with SfM-estimated plant height, with slight differences in plot positions between 2022 and 2023. Yields in 2023 tended to be lower for plants that were similar in height, and the number of harvests was also fewer. Possible reasons for these annual differences include variations in weather

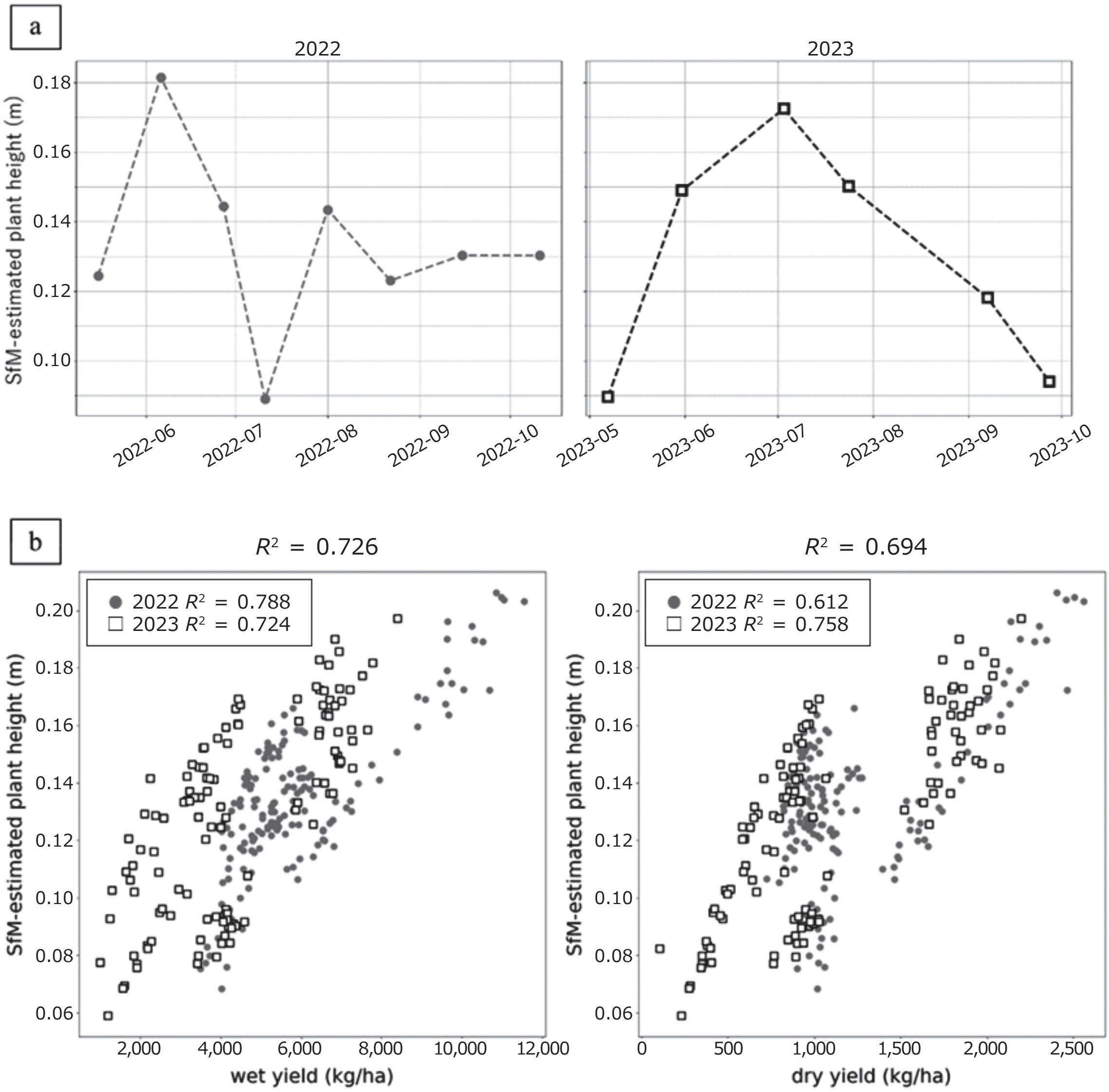

Fig. 2. SfM-estimated plant height

(a) Temporal dynamics of plant height across the observation period. (b) Relationships between plant height and yield: left, wet (fresh-matter) yield; right, dry-matter yield. Coefficients of determination (R^2) shown above each panel (outside the frame, top-center) are for the pooled two-year dataset; R^2 values shown within panels (top-left) are year-specific.

conditions and the number of overwintering cycles. The average temperature in August was 22.7°C in 2022 and 26.7°C in 2023 (a 4°C difference), suggesting that the higher temperatures in August 2023 adversely affected the growth of *L. perenne*, a cool-season grass sensitive to heat stress. The interval between the fourth and fifth harvestings in 2023, which included August, was significantly longer at 45 days, than the average of 21 days in 2022. Additionally, total precipitation in August 2022 was 233 mm, compared to approximately 69.5 mm in August 2023 (Fig. 3). These differences in weather conditions may have contributed to the observed differences in the growth of *L. perenne* between the two years. The study site, in Sapporo City, Hokkaido, is characterized by extensive snow cover during winter, which, along with low temperatures, influences plant growth after overwintering. Cumulative damage caused by repeated overwintering is also considered a contributing factor.

2. Yield estimation of *Lolium perenne*

Table 3 shows yield estimation results using SfM-estimated plant height, temperature, and precipitation. Yield estimation was carried out using SfM-estimated plant height as a base, both alone and in combination with one or more meteorological items. Conditions where training and test data were from the same year (2022, 2023, 2022+2023 datasets) showed significantly higher R^2 values and lower MAPE values than conditions where different years were used for training and testing (2022→2023, 2023→2022). The reduced accuracy in the latter is likely attributable to inter-annual variations in weather and growth patterns, which rendered models trained on one year's data ineffective for predicting the other year's yield. It should also be noted that the data partitioning approach differed between the 2022, 2023, 2022+2023 models and the 2022→2023, 2023→2022 models, which may have partially contributed to the observed difference in accuracy. This interpretation is supported by the low or negative R^2 values observed. When the training and test datasets were from the same year, including weather data improved both R^2 and MAPE compared to models using plant height alone. Temperature and precipitation, which are significant factors influencing annual crop growth, are routinely recorded at observation sites and are therefore readily available for yield estimation models. Incorporating these variables can improve accuracy,

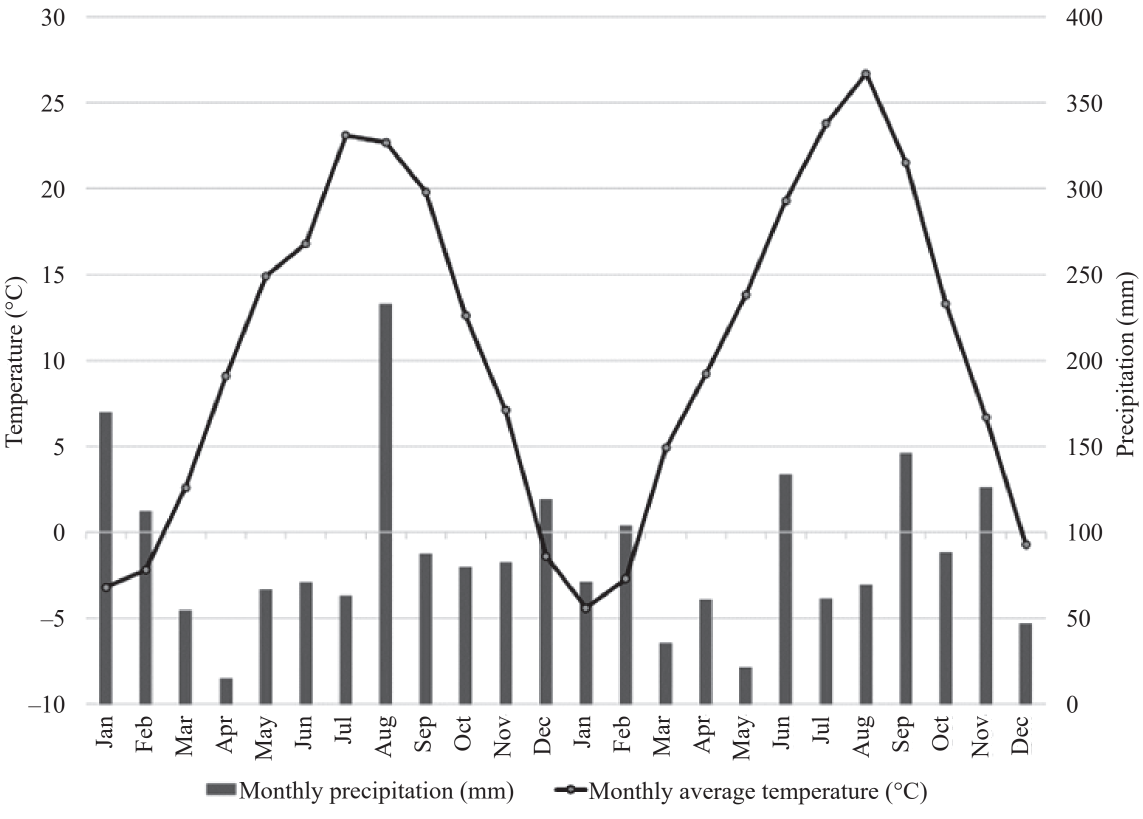

Fig. 3. Monthly changes of mean air temperature and precipitation between 2022 and 2023

especially under conditions such as those in this study, where frequent harvests occur over short intervals.

Adding vegetation indices as explanatory variables resulted in minimal changes in R^2 and MAPE compared with the inclusion of temperature and precipitation. No vegetation index consistently improved accuracy across all data partitioning conditions. The limited efficacy of vegetation indices in this study may be attributed to the use of multi-temporal data, variations in weather and lighting conditions during image acquisition, and lighting inconsistencies within the orthomosaic images used for analysis. Consequently, vegetation indices were potentially unsuitable as multi-timepoint growth indicators for yield estimation under these conditions. However, previous studies have reported improved estimation accuracy when vegetation indices derived from RGB images were included as explanatory variables in addition to plant height (Viljanen et al. 2018, Pranga et al. 2021). While these studies focused on UAV-based biomass estimation in controlled experimental or research station settings, the present study examines the applicability of UAV-SfM-derived plant height for yield estimation under breeding trial conditions. This practical perspective highlights operational challenges and considerations for applying UAV-SfM in real-world breeding contexts. To enhance the potential utility of vegetation indices, it may be beneficial to minimize differences in weather conditions during image acquisition as much as possible, capture images that cover the entire field in a single shot separately from those used for SfM processing, and use these images exclusively for vegetation index calculation.

Given the large margin of error observed in the results, the accuracy is considered insufficient for practical application in breeding productivity trials, where a yield difference of 5% between varieties is considered significant. This study was conducted under a limited set of conditions, resulting in a relatively small dataset. The dataset size (20 plots per year) is admittedly small for machine learning-based modeling. Although cross-year validation was employed to assess generalizability, future studies should aim to include larger and more diverse datasets across multiple locations and years to improve model robustness and generalizability. Furthermore, inter-annual differences in growth had a marked impact on estimation accuracy. To improve accuracy and develop a more robust, versatile model, it is necessary to collect additional data across a broader range of conditions. Additionally, exploring the inclusion of other explanatory variables and evaluating alternative modeling approaches, such as support vector machines, artificial neural networks, or partial least squares regression alongside RF, may be beneficial, especially to improve generalizability across years.

3. SfM-estimated plant height and rG in individual selection

The relationship between UAV-SfM-estimated plant height and rG is shown in Figure 4. A strong correlation of 0.841 was observed between the two variables. The

Table 3. Yield prediction performance using Structure-from-Motion (SfM)-derived plant height (PH), temperature (T), and precipitation (P) as explanatory variables

	Plant height（PH）				PH_Temperature (T)			
	Wet yield		Dry yield		Wet yield		Dry yield	
	R^2	MAPE	R^2	MAPE	R^2	MAPE	R^2	MAPE
2022	0.61	13.9	0.44	19.1	0.95	5.4	0.97	5.1
2023	0.48	30.4	0.51	34.6	0.95	9.3	0.97	10.1
2022＋2023	0.41	28.4	0.39	31.6	0.96	7.0	0.93	8.7
2022→2023	–0.23	57.5	0.20	59.8	0.04	58.3	0.14	62.8
2023→2022	–0.43	29.6	–0.18	33.7	0.24	24.9	–0.01	35.7
	PH_Precipitation (P)				PH_T_P			
	Wet yield		Dry yield		Wet yield		Dry yield	
	R^2	MAPE	R^2	MAPE	R^2	MAPE	R^2	MAPE
2022	0.89	6.0	0.86	7.5	0.95	5.1	0.97	4.9
2023	0.95	9.7	0.96	10.9	0.95	9.2	0.97	10.1
2022＋2023	0.93	7.6	0.90	9.4	0.96	6.6	0.93	8.1
2022→2023	0.08	51.2	0.66	37.5	0.04	58.0	0.41	45.8
2023→2022	–0.73	32.2	–0.11	26.6	0.20	24.4	0.22	31.0

concentration of points in the top-right region of the plot is attributable to the large number of relatively well-growing individuals, whose similar growth conditions resulted in closely clustered data points. Over time, as leaf growth progresses, individuals with greater height and leaf area increase, leading to higher UAV-SfM-estimated plant height and rG values. Consequently, the distribution of points is expected to become increasingly biased toward the top-right region, potentially reducing the correlation coefficient. Excessive plant height may also lead to lodging, compromising the reliability of the UAV-SfM-estimated plant height. In the case of rG, a large variation in growth may reduce the ability to distinguish differences within well-growing groups. Additionally, as plant density increases, the analysis area becomes dominated by leaves, reducing the differentiation of GRVI values. Furthermore, expanding leaves may encroach upon the analysis areas of neighboring individuals, leading to estimates that do not accurately represent a single plant. For these reasons, when using UAV-SfM-estimated plant height or rG for individual selection, careful consideration of the optimal timing for aerial imagery is necessary to ensure measurement accuracy.

It has previously been demonstrated that rG exhibits a strong positive correlation with breeder evaluations used for individual selection. In this study, a strong correlation was observed between rG and UAV-SfM-estimated plant height, suggesting that UAV-SfM-estimated plant height may also be useful for individual selection. Since the rG index is calculated using only RGB values, it cannot reflect 3D information. In contrast, UAV-SfM estimated plant height incorporates 3D; however, because the SfM-generated 3D point cloud primarily represents the outer surface of the plants, it cannot capture details such as leaf density. By combining these two indices, it may be possible to compensate for each index's limitations, thereby improving the accuracy of individual selection. Although this study demonstrated a high correlation between rG and UAV-SfM-derived plant height, suggesting the potential of a combined index for more effective selection, the practicality of SfM in routine breeding operations may currently be limited due to cost and labor. Therefore, the use of rG alone could be sufficient for practical selection purposes in many field settings.

4. Conclusion

This study examined the application of UAV-SfM-estimated plant height for yield estimation and individual evaluation in grass breeding selection. While yield estimation using UAV-SfM estimated plant height did not achieve the accuracy required for application in breeding productivity trials, the potential utility of UAV-SfM-estimated plant height for individual selection remains promising. Further research is needed to expand the dataset and examine the applicability of this approach to other crops and fields under different conditions. This study assessed the feasibility of existing estimation technology in breeding fields.

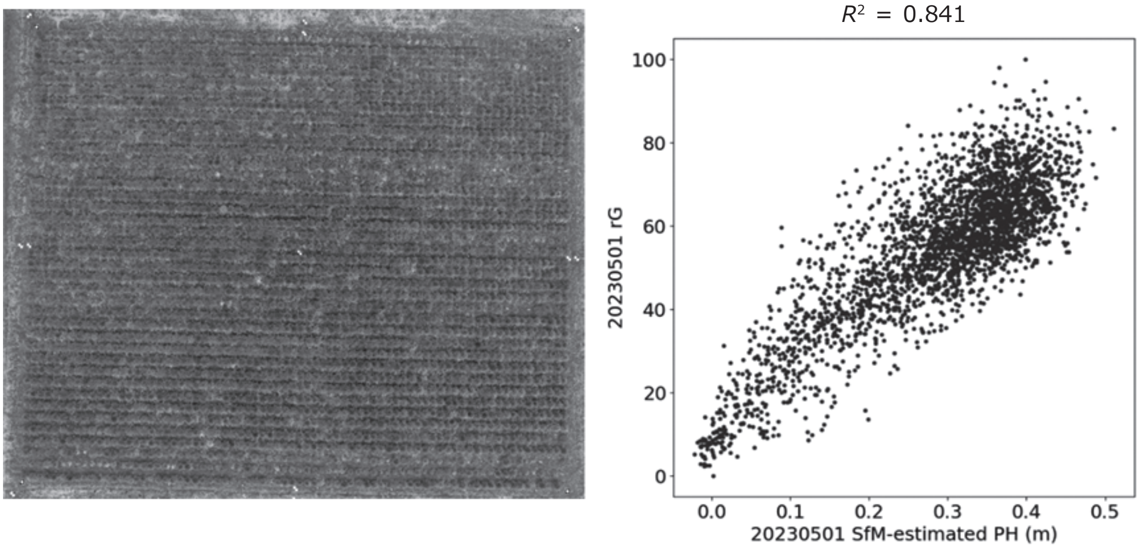

Fig. 4. Plot of SfM-estimated plant height and rG

On the left is an image of the entire field containing 2,886 individuals, captured from a height of 40 m on 1 May 2023. The R^2 at the top center of the right plot is the correlation coefficient.

Acknowledgements

This research was supported by JSPS KAKENHI Grant Number JP23K05197 and the research program on development of improved crop varieties for food security grants from the Project of the Bio-oriented Technology Research Advancement Institution (BRAIN) Grant Number JPJ012082.

References

Akiyama, Y. et al. (2019) Development of a New Evaluation Method for Individual Selection in Grass Breeding with Unmanned Aerial Vehicle (UAV) and Image Analysis. *Nihon sochi gakkaishi* (*Jpn. J. Grassl. Sci.*), **65**, 8-14 [In Japanese with English summary].

Bendig, J. et al. (2015) Combining UAV-based plant height from crop surface models, visible, and near infrared vegetation indices for biomass monitoring in barley. *Int. J. Appl. Earth Obs. Geoinf.*, **39**, 79-87.

Cook, K. L. & Dietze, M. (2019) A simple workflow for robust low-cost UAV-derived change detection without ground control points. *Earth Surf. Dyn.*, **7**, 1009-1017.

da Silva, A. K. V. et al. (2021) Predicting Eucalyptus Diameter at Breast Height and Total Height with UAV-Based Spectral Indices and Machine Learning. *Forests*, **12**, 582.

Galli, G. et al. (2021) A novel way to validate UAS-based high-throughput phenotyping protocols using in silico experiments for plant breeding purposes. *Theor. Appl. Genet.*, **134**, 715-730.

Grüner, E. et al. (2019) Biomass prediction of heterogeneous temperate grasslands using an SfM approach based on UAV imaging. *Agronomy*, **9**, 54.

Kikawada, T. et al. (2022) Comparison of green red vegetation index (GRVI) with other RGB vegetation indices in forage crop breeding. *Ikushugaku kenkyu* (*Breed. Res.*), **24**, 134-145 [In Japanese with English summary].

Kikawada, T. et al. (2024) Effectiveness of Pasture Selection Using Vegetation Index rG (relative Green Red Vegetation Index) and Comparison with Conventional Selection Methods. *Nihon sochi gakkaishi* (*Jpn. J. Grassl. Sci.*), **70**, 1-9 [In Japanese with English summary].

Li, W. et al. (2016) Remote estimation of canopy height and aboveground biomass of maize using high-resolution stereo images from a low-cost unmanned aerial vehicle system. *Ecol. Indic.*, **67**, 637-648.

Malambo, L. et al. (2018) Multitemporal field-based plant height estimation using 3D point clouds generated from small unmanned aerial systems high-resolution imagery. *Int. J. Appl. Earth Obs. Geoinf.*, **64**, 31-42.

Pranga, J. et al. (2021) Improving accuracy of herbage yield predictions in perennial ryegrass with UAV-based structural and spectral data fusion and machine learning. *Remote Sens.*, **13**, 3459.

Viljanen, N. et al. (2018) A novel machine learning method for estimating biomass of grass swards using a photogrammetric canopy height model, images and vegetation indices captured by a drone. *Agriculture*, **8**, 70.

Wang, J. et al. (2019) Using sensors and unmanned aircraft systems for high-throughput phenotyping of biomass in perennial ryegrass breeding trials. *Front. Plant Sci.*, **10**, 1381.

Wang, L. et al. (2016) Estimation of biomass in wheat using random forest regression algorithm and remote sensing data. *Crop J.*, **4**, 212-219.